Biochemical and Biophysical Research Communications 458 (2015) 418–423

Contents lists available at ScienceDirect

Biochemical and Biophysical Research Communications

journal homepage: www.elsevier.com/locate/ybbrc

Steady-state and time-resolved Thioflavin-T fluorescence can report on morphological differences in amyloid fibrils formed by Aβ(1-40) and Aβ(1-42)

David J. Lindberg [a], Moa S. Wranne [b], Mélina Gilbert Gatty [b], Fredrik Westerlund [a], Elin K. Esbjörner [a, *]

[a] Department of Biology and Biological Engineering, Division of Chemical Biology, Chalmers University of Technology, Kemivägen 10, SE-41296 Gothenburg, Sweden
[b] Department of Chemistry and Chemical Engineering, Division of Physical Chemistry, Chalmers University of Technology, Kemivägen 10, SE-41296 Gothenburg, Sweden

ARTICLE INFO

Article history:
Received 13 January 2015
Available online 7 February 2015

Keywords:
Amyloid-β
Amyloid fibrils
Alzheimer's disease
Thioflavin-T
Amyloid dye
Fluorescence lifetime

ABSTRACT

Thioflavin-T (ThT) is one of the most commonly used dyes for amyloid detection, but the origin of its fluorescence enhancement is not fully understood. Herein we have characterised the ThT fluorescence response upon binding to the Aβ(1-40) and Aβ(1-42) variants of the Alzheimer's-related peptide amyloid-β, in order to explore how the photophysical properties of this dye relates to structural and morphological properties of two amyloid fibril types formed by peptides with a high degree of sequence homology. We show that the steady-state ThT fluorescence is 1.7 times more intense with Aβ(1-40) compared to Aβ(1-42) fibrils in concentration matched samples prepared under quiescent conditions. By measuring the excited state lifetime of bound ThT, we also demonstrate a distinct difference between the two fibril isoforms, with Aβ(1-42) fibrils producing a longer ThT fluorescence lifetime compared to Aβ(1-40). The substantial steady-state intensity difference is therefore not explained by differences in fluorescence quantum yield. Further, we find that the ThT fluorescence intensity, but not the fluorescence lifetime, is dependent on the fibril preparation method (quiescent versus agitated conditions). We therefore propose that the fluorescence lifetime is inherent to each isoform and sensitively reports on fibril microstructure in the protofilament whereas the total fluorescence intensity relates to the amount of exposed β-sheet in the mature Aβ fibrils and hence to differences in their morphology. Our results highlight the complexity of ThT fluorescence, and demonstrate its extended use in amyloid fibril characterisation.

1. Introduction

Amyloid formation is associated with many protein deposition disorders, including severely debilitating neurodegenerative diseases [1]. A primary pathological hallmark of Alzheimer's disease (AD), is the formation of senile plaques consisting of fibrillar forms of the amyloid-β peptide (Aβ) [2]. Aβ exists in several isoforms; the most abundant *in vivo* is the 40-residue Aβ(1-40) peptide whilst the 42-residue Aβ(1-42) peptide is the major proteinaceous component of senile plaques [3,4].

Amyloid fibrils formed from different proteins share common characteristics; they form long twisted filaments with diameters of the order of 10 nm and share a common cross-β structure with β-strands oriented perpendicular to the fibril long axis [5]. Due to these similarities, the cross-β structure of most fibrils can accommodate specific stains such as Thioflavin-T (ThT), which is routinely used to recognize amyloid fibrils *in vitro*, *ex situ* and in histological samples [6,7]. Despite wide-spread use, the binding mode of ThT to amyloid fibrils, and the origin of its enhanced fluorescence upon binding remains debated. It appears that ThT preferentially binds in the "channels" formed between adjacent side-chains protruding from the amyloid core, and running parallel to the fibril long axis [8]. ThT may have a certain interaction preference for aromatic side chains and the dye also interacts with the aromatic-rich active site of folded acetylcholine esterase [9–11].

* Corresponding author.
E-mail address: eline@chalmers.se (E.K. Esbjörner).

http://dx.doi.org/10.1016/j.bbrc.2015.01.132

ThT is a so-called molecular rotor; in water its excitation energy rapidly dissipates through rotation around the central carbon bond (Fig. 1A), resulting in a short fluorescence lifetime and low quantum yield [12–14]. In amyloid fibrils, this rotation becomes restricted due to geometric constraints in the binding site. This results in an increased quantum yield [15]. However, ThT intensities differ significantly between amyloid samples, even between fibrils formed from single mutant isoforms of the same protein [16,17]. This intensity-fibril relationship is not well documented, and often overlooked by normalization of emission data. Yet, the magnitude of ThT fluorescence enhancement upon fibril binding could contain useful information on fibril structure. Since ThT binds to exposed β-sheet regions, its fluorescence response could potentially be used to detect and differentiate different surface features of amyloid fibrils. This information is useful, particularly since the surface of amyloid fibrils and plaque deposits appear to catalyse fibril formation by promoting secondary nucleation in fibril forming reactions [18,19].

Amyloid fibrils formed by different Aβ variants differ significantly in their ability to enhance ThT emission [16,17], despite high sequence homology and several apparent similarities in the architecture of the β-hairpins that build their amyloid cores [20–27] (see schematic in Fig. 1B). Here we have studied photophysical features of ThT bound to Aβ(1-40) and Aβ(1-42) fibrils in order to understand how these differences relate to structure and morphology of the respective fibrils and to explore the potential extended use of ThT as a structural amyloid probe.

2. Materials and methods

2.1. Peptide handling and amyloid formation

Lyophilized powders of recombinant Aβ(1-40) and Aβ(1-42) (AlexoTech AB) were dissolved in 10 mM NaOH to a concentration of 1 mg/ml. The solutions were aliquoted, snap-frozen and stored at −80 °C until further use. Fibrillar Aβ(1-40) or Aβ(1-42) was prepared by diluting aliquots in 50 mM sodium phosphate buffer (pH 7.4) followed by incubation for 96 h in quiescent conditions or 48 h using 800 rpm orbital shaking.

2.2. Aβ concentration determination

The concentration of monomeric Aβ(1-40) and Aβ(1-42) before and after fibrillation was determined using a modified bicinchoninic acid (BCA) assay (Pierce). Residual monomers were separated from formed fibrils by centrifugation at 13,000 rpm for 10 min to pellet the fibrils. BCA assay reagents were added and the absorbance of each sample was read at 544 nm after 2 h incubation at 37 °C. Bovine serum albumin (BSA) was used as standard. To account for the smaller hydrodynamic radius of Aβ compared to BSA, the standard curve was corrected by a factor of 0.766 (Fig. S1) [28].

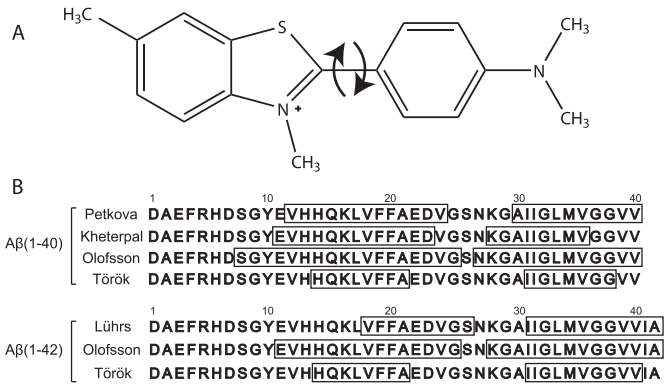

Fig. 1. A: Chemical structure of Thioflavin-T, with arrows showing rotational movement around the central carbon bond. B: Sequence of Aβ(1-40) and Aβ(1-42), with boxes showing possible regions of β-sheet formation as determined by previous studies [20–27].

2.3. Steady-state fluorescence spectroscopy

Fluorescence spectra were recorded on a Varian Eclipse fluorimeter (Agilent Technologies) using a 60 μl quartz cuvette with 3 mm path length (Hellma). Emission spectra were collected between 450 and 600 nm upon excitation at 440 nm, and excitation spectra between 400 and 470 nm using an emission wavelength of 485 nm. The averaging time was 300 ms and the excitation and emission monochromator slit widths were 5 and 10 nm respectively.

2.4. Time-resolved fluorescence

Fluorescence lifetimes were measured by time correlated single photon counting. A pulsed (10 MHz) laser diode emitting at 405 nm (PicoQuant) was used for excitation. Emitted photons were collected at 485 ± 10 nm by an R3809U-50 microchannel-plate photomultiplier tube (Hamamatsu) and fed into a Lifespec multichannel analyser (Edinburgh Analytical Instruments) with its time window set to 50 ns divided into 2048 channels. 10,000 counts were recorded in the top channel. The data was fitted by a Levenberg–Marquardt non-linear least squares method using PicoQuant FluoFit software.

2.5. Circular dichroism (CD)

CD spectra were recorded between 190 and 300 nm on a Chirascan spectropolarimeter (Applied Photophysics) using a quartz cuvette with 1 mm path length (Hellma). The bandwidth was 1 nm and the collection time 500 ms. Five spectra were recorded and averaged. Spectra were corrected for background contributions by subtracting buffer blanks, smoothed by a five-point Savitsky–Golay algorithm and normalized to have a maximum negative value of −1 in order to best compare spectral shapes.

2.6. Atomic force microscopy (AFM)

Fibrillar Aβ(1-40) or Aβ(1-42) were deposited on freshly cleaved mica. After 5 min, the mica was rinsed with filtered milli-Q water and dried under a gentle nitrogen stream. Images were recorded on an NTEGRA Prima setup (NT-MDT) using a gold-coated single crystal silicon cantilever (NT-MDT, NSG01, spring constant of ~5.1 N/m) and a resonance frequency of ~150 kHz. 1024 pixel 10 × 10 μm images were acquired with 0.5 Hz scan rate. Fibrillar heights were determined from the AFM images as detailed in the supporting information.

3. Results

3.1. Fibril yields in Aβ(1-40) and Aβ(1-42) aggregation reactions

ThT emission intensities are commonly assumed to correlate to the amount of amyloid fibrils in a sample and differences between samples could therefore be a consequence of that the amyloid fibril reactions have reached different equilibria, i.e. have proceeded with different yields. To exclude this trivial explanation to previously observed differences in end-point ThT emission intensities in fibril forming reactions with Aβ(1-40) and Aβ(1-42) [16,17] we first determined the fibril yields under our experimental conditions. We

determined the peptide concentration before and after aggregation of Aβ(1-40) and Aβ(1-42) under quiescent or agitated conditions, by separating the fibrillar material from residual monomers. We found that both Aβ(1-40) and Aβ(1-42) form fibrils with yields in the order of ~90% and that the initial peptide concentrations (determined by gravimetric analysis) differed by less than 10% (Table 1, Fig. S2).

3.2. Steady-state emission of ThT bound to fibrils of Aβ(1-40) and Aβ(1-42)

Having shown that we can prepare fibrillar samples of Aβ(1-40) and Aβ(1-42) with equal concentration and negligible residual monomer content, we added ThT in 2-fold molar excess and recorded the steady-state fluorescence emission. At this concentration (close to emission saturation in both cases (Fig. S3)) we found that the Aβ(1-40) fibrils prepared in quiescent conditions enhance the ThT emission 1.7 times more efficiently than Aβ(1-42) fibrils (Fig. 2A). This suggests profound structural differences between the two fibril types. Since it is common to use agitation to enhance amyloid formation we also investigated if the conditions under which the Aβ(1-40) and Aβ(1-42) fibrils were formed influence the ThT emission intensity. Comparing Aβ(1-40) and Aβ(1-42) fibrils formed under agitation therefore we still observe a higher emission intensity of ThT bound to Aβ(1-40) fibrils, but the difference is now smaller (1.25-fold) (Fig. 2A). Interestingly, agitation therefore appears to have a larger effect on Aβ(1-40) fibrils than on Aβ(1-42) fibrils. We observed no differences in the shape of ThT emission spectra between different samples, whereas the excitation spectra showed clearly different maxima (Fig. 2B, Table 1). Upon binding to amyloid fibrils the ThT absorption exhibits a significant red-shift from 412 nm in water to typically 440–450 nm. Our results show that this red-shift is larger for Aβ(1-40) fibrils (36–38 nm) compared to Aβ(1-42) fibrils (32–34 nm), possibly indicating some minor difference in the degree of planarization of the bound ThT dye [14].

3.3. Fluorescence lifetimes of ThT bound to Aβ(1-40) and Aβ(1-42) fibrils

We next examined the fluorescence lifetime of fibril-bound ThT in order to better understand the origin of the abovedescribed intensity variances. Fig. 3A shows typical fluorescence decays of ThT in presence of the different Aβ fibrils examined above. The decays are multi-exponential, as has previously been observed in viscous solvents [15]. It was necessary to use three exponentials to accurately fit the measured data. The decay of unbound ThT in buffer was adequately fitted to a double-exponential (Fig. S4). As it was not possible to assign the individual lifetime components to molecular conformations we report all fluorescence lifetimes by their intensity-weighted average (Table 2). The decays and the associated lifetimes of ThT are distinctly different for Aβ(1-40) and Aβ(1-42) fibrils; the fluorescence lifetime of ThT is always longer in samples with Aβ(1-42) fibrils. This suggests that the local physicochemical environment of the ThT binding sites in Aβ(1-40) and Aβ(1-42) fibrils are different, despite that their primary sequences only differ by two additional hydrophobic amino acids in the C-terminus of Aβ(1-42), as will be further discussed below. Interestingly, the ThT fluorescence lifetime is not affected by changes to the aggregation conditions (quiescent versus agitation), indicating that Aβ(1-40) and Aβ(1-42) fibrils can be associated with a certain ThT fluorescence lifetime, irrespective of the conditions under which they were formed. We propose that this fluorescence lifetime can therefore be a signature of a specific Aβ fibril isoform.

Table 1
Monomer Aβ concentrations of supernatant as measured by BCA concentration assay before and after aggregation, including excitation maximum of bound ThT.

Sample	Incubation	Pre aggregation (μM)	Post aggregation (μM)	Fibril yield	Ex max (nm)
$A\beta_{1-40}$	Quiescent	36.7	3.0 ± 0.8	92%	450
$A\beta_{1-40}$	Agitated	36.7	4.9 ± 2.0	87%	448
$A\beta_{1-42}$	Quiescent	40.2	3.6 ± 0.8	91%	444
$A\beta_{1-42}$	Agitated	40.2	3.4 ± 1.7	92%	446

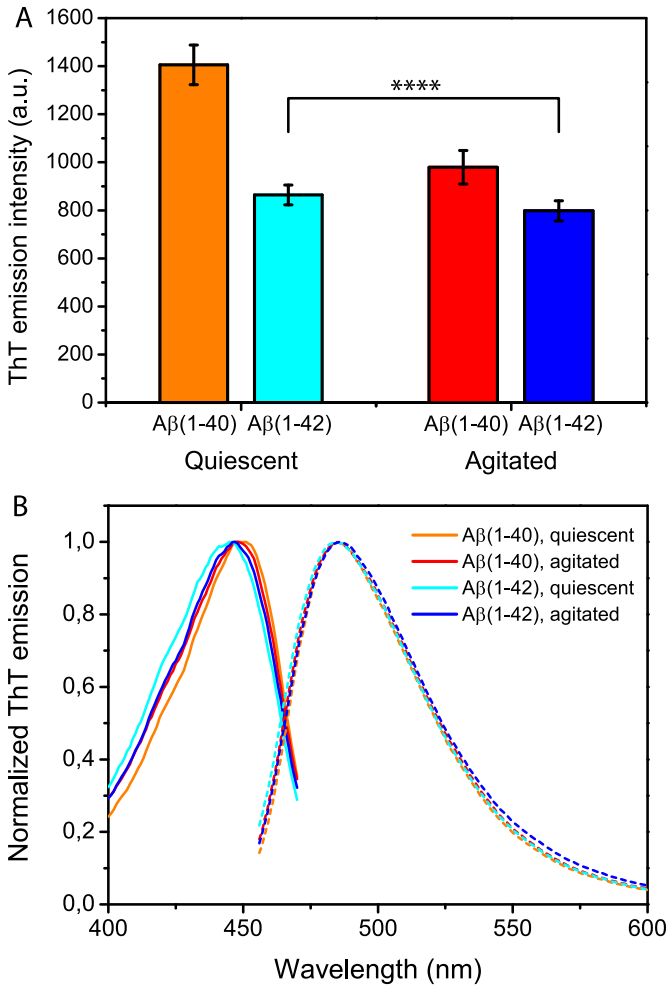

Fig. 2. A: Steady state Thioflavin T fluorescence emission in presence of Aβ(1-40) and Aβ(1-42) amyloid fibrils. 60 μM thioflavin-T with: Orange) 27.0 μM Aβ(1-40) fibrils formed under quiescent conditions. Cyan) 29.3 μM Aβ(1-42) fibrils formed under quiescent conditions. Red) 25.4 μM Aβ(1-40) fibrils formed under agitated conditions. Blue) 29.4 Aβ(1-42) fibrils formed under agitated conditions. (****$p < 0.0001$) B: Normalized steady-state excitation and emission spectra of ThT in presence of Aβ(1-40) and Aβ(1-42) fibrils. 60 μM thioflavin-T with: Orange) 27.0 μM Aβ(1-40) fibrils formed under quiescent conditions. Cyan) 29.3 μM Aβ(1-42) fibrils formed under quiescent conditions. Red) 25.4 μM Aβ(1-40) fibrils formed under agitated conditions. Blue) 29.4 Aβ(1-42) fibrils formed under agitated conditions. Data in both figures represents the average value of three independent experiments each performed in triplicate ($N = 3$, $n = 3$) with error bars showing the standard deviation. (For interpretation of the references to colour in this figure caption, the reader is referred to the web version of this article.)

3.4. Secondary structure and morphology of Aβ(1-40) and Aβ(1-42) fibrils

We examined the Aβ fibrils by CD spectroscopy to assess their secondary structure (Fig. 3B). All Aβ fibrils have expected

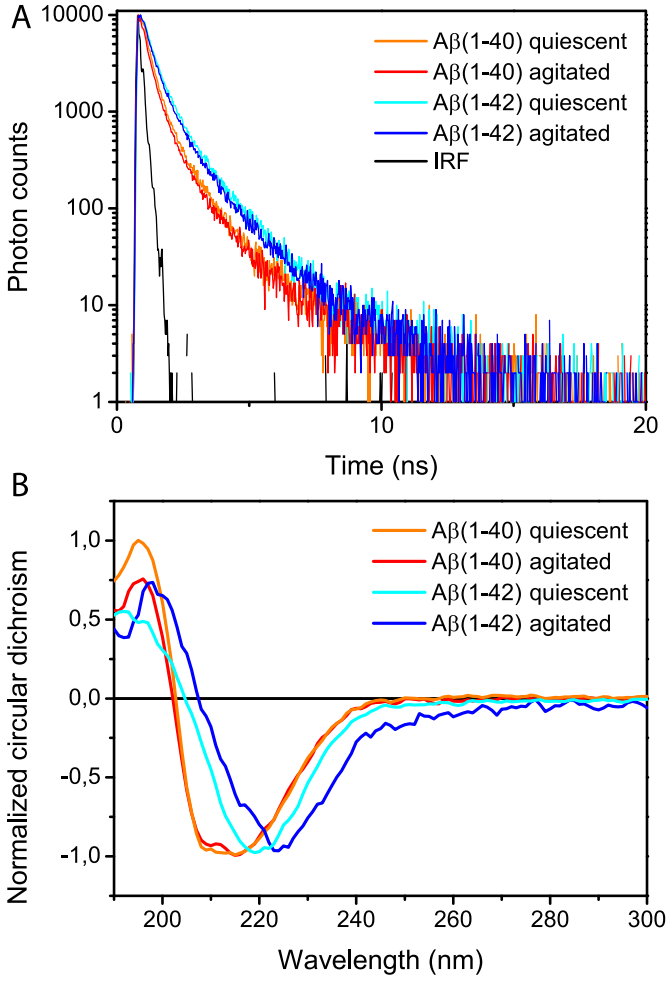

Fig. 3. A: Fluorescence emission decay curves of ThT bound to Aβ fibrils. The ThT concentration was always 60 μM and the traces correspond to: Orange) 27.0 μM $Aβ_{1-40}$ fibrils formed under quiescent conditions. Red) 25.4 μM $Aβ_{1-40}$ fibrils formed under agitated conditions. Cyan) 29.3 $Aβ_{1-42}$ fibrils formed under quiescent conditions. Blue) 29.4 $Aβ_{1-42}$ fibrils formed under agitated conditions. The instrument response function (IRF) is shown in black. B: Circular dichroism spectra of $Aβ_{1-40}$ and $Aβ_{1-42}$ amyloid fibrils. Normalized far UV circular dichroism spectra of $Aβ_{1-40}$ fibrils formed under quiescent (orange) or agitated (red) conditions and of $Aβ_{1-42}$ formed under quiescent (blue) or agitated (cyan) conditions. The spectra were normalized by division of the negative maximum. All curves were smoothed using a five-point Savitsky-Golay algorithm. Non-normalized spectra are provided in the supporting information (Fig. S5). (For interpretation of the references to colour in this figure caption, the reader is referred to the web version of this article.)

predominant β-structure as shown by the negative peaks in the 215–220 nm region and positive peaks around 196 nm. There are slight differences in the shape of the CD spectra of the Aβ(1-40) and Aβ(1-42) fibrils; the latter spectra exhibit sharper and somewhat red-shifted negative peaks; the differences are however too small to explain the large differences in emission intensity.

We also used AFM to examine the morphology of the different fibrils. Fig. 4A shows that Aβ(1-40) forms very long fibrils, often extending more than 10 μm in length, whereas Aβ(1-42) forms considerably shorter fibrils; typically in the range of 3–4 μm or less. More importantly, however, the fibrils also differ with respect to fibril height (Fig. 4B, Fig. S6); Aβ(1-40) fibrils are thinner and more homogeneous in their fibril height distribution compared to Aβ(1-42) fibrils. In addition, Aβ(1-40) fibrils are less laterally associated than Aβ(1-42) fibrils. Agitation is known to cause fibril fragmentation, resulting in shorter fibrils [29], which we do observe for Aβ(1-42). For Aβ(1-40) fibrils such effects are less clear since their

Table 2
Fluorescence lifetimes calculated from multi-exponential fits of ThT emission decay curves. All lifetimes were averaged from triple-exponential fits, except free ThT which was fitted to a double-exponential decay (Fig. S4).

Sample	Incubation	$<\tau>^a$	χ^2
$Aβ_{1-40}$	Quiescent	0.43	1.272
$Aβ_{1-40}$	Agitated	0.44	1.128
$Aβ_{1-42}$	Quiescent	0.63	1.084
$Aβ_{1-42}$	Agitated	0.61	1.081

[a] Intensity-weighted average emission lifetime.

lengths often exceeded the size of the AFM scan area. Shaking of the Aβ(1-40) fibrils leads, however, to increased formation of clustered or laterally associated fibrils (Fig. S7) although the extent of this effect was difficult to quantify.

4. Discussion

Characterization of the structural and physicochemical properties of amyloid fibrils is important for understanding how these aggregates are involved in disease. For example, recent studies of Aβ fibril formation have revealed that the proliferation of fibrillar aggregates is highly dependent on secondary nucleation [18,19,30], which highlights that fibril morphology and the nature of the solvent exposed fibril is important in catalysing the formation of new amyloid aggregates. Conformation-specific antibodies [31] and luminescent conjugated polymers [32] are examples of new tools that have been developed to probe such fibril properties. Our study shows, however, that also ThT, the perhaps most commonly used amyloid dye, can report valuable information on subtle variations in fibril structure and distinguish between different fibril types.

We report that the ThT emission intensity differs significantly between samples containing fibrillar Aβ(1-40) and Aβ(1-42) and show that this difference is not related to fibril yield; a factor that would for example reduce ThT intensity in presence of an amyloid inhibitor. We further observe that Aβ fibrils formed under agitation differ from those formed under quiescent conditions with respect to their ability to enhance ThT emission; this is particularly evident for Aβ(1-40) fibrils where agitation results in ~25% emission reduction in concentration-matched samples. This finding suggests that agitation affects fibril morphology, a conclusion that is also supported by AFM data, but moreover it shows that ThT can sensitively report on such changes. Differences in ThT intensity between fibril samples could for example be due to that fibrils can accommodate different amounts of ThT (i.e. have different numbers of available binding sites), that the affinity of each binding site is different, or that the ThT molecules bound to the different fibrils have different fluorescence quantum yields (brightness).

We report a difference in ThT fluorescence lifetime between Aβ(1-40) and Aβ(1-42) fibrils, supporting that ThT molecules bound to the different fibrils do have different quantum yields and thus different inherent brightness. However, since the fluorescence lifetime of ThT is shorter with Aβ(1-40) fibrils than with Aβ(1-42) fibrils this contradicts the higher emission intensity in Aβ(1-40) fibrils, and shows that the intensity differences cannot be explained simply as a difference in quantum yield. Further, we cannot detect any marked differences in the binding affinity of ThT to Aβ(1-40) and Aβ(1-42) fibrils (Fig. S3). Therefore, our data suggest that Aβ(1-40) and Aβ(1-42) fibrils foremost differ in their capacity to accommodate ThT, i.e. Aβ(1-40) fibrils appear to have more available binding sites, thereby enabling them to bind more ThT molecules than Aβ(1-42) fibrils explaining the higher ThT emission intensity. Neither our CD data nor published structural models (see cartoon in Fig. 1B) support that Aβ(1-40) fibrils would have more

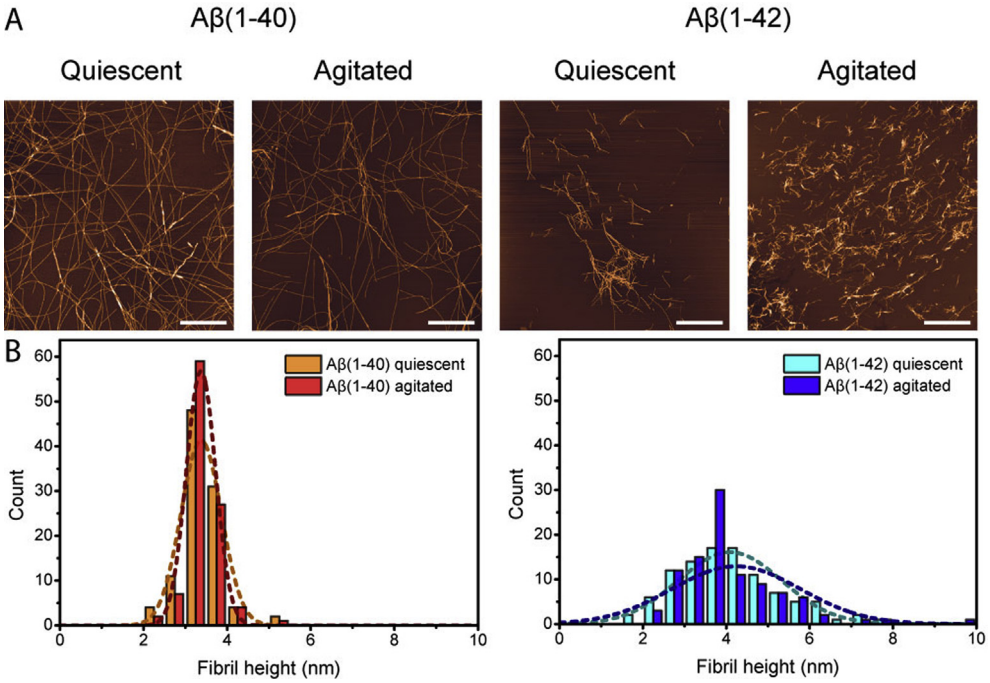

Fig. 4. A: AFM micrographs of, from left to right: Aβ(1-40) fibrils formed under quiescent conditions, Aβ(1-40) fibrils formed under agitated conditions, Aβ(1-42) fibrils formed under quiescent conditions and Aβ(1-42) fibrils formed under agitated conditions. All scale bars are 2 μm. B: Fibril height histograms of left: Aβ(1-40) fibrils formed under quiescent or agitated conditions, right: Aβ(1-42) fibrils formed under quiescent or agitated conditions. Dashed curves represent gaussian distributions fitted to the corresponding histogram.

binding sites due to a significantly more extended cross-β core. Moreover, a study of ThT binding to HET-s fibrils strongly suggest that only a small fraction of the "channels" exposed on the fibril surface are in fact accessible to ThT [33]. Instead we propose, with support from AFM data, that Aβ(1-40) fibrils, due to their thin morphology and low tendency of lateral association can accommodate more ThT molecules because of their overall architecture. Interfilament contacts may allow them to expose more β-sheet on the surface of the fibril, whereas in Aβ(1-42) fibrils the β-sheet regions may be less accessible due to more extensive interfilament interactions but also lateral association of mature fibrils. The observation that shaking reduces ThT emission of the formed fibrils is consistent with this explanation as we find that this results in a higher degree of lateral association, particularly for the Aβ(1-40) fibrils (Fig. S7).

An important conclusion from this work is that the ThT fluorescence lifetime can be considered a signature of each of the Aβ isoforms and that its value is invariant to the aggregation conditions. This shows that the ThT binding site is conserved and implies that the microscopic structure of each Aβ fibril is indifferent to agitation. An intriguing consequence is that the ThT lifetime could be used to recognize and distinguish between different fibril types in more complex samples.

Aβ(1-40) and Aβ(1-42) differ only by two additional C-terminal hydrophobic residues in Aβ(1-42). This difference does affect the structure and morphology of the resulting amyloid fibrils primarily by extending the second β-sheet in the Aβ hairpin. Molecular dynamics simulations with short Aβ segments have shown that ThT preferentially binds in a channel in between phenylalanine and valine on an exposed EFVK face [34]. In the full length peptides this channel is between residues V18 and F20. Structural models suggest that this channel is in the centre of the first β-sheet of the Aβ hairpin and therefore solvent-exposed in both Aβ(1-40) and Aβ(1-42) fibrils. It is therefore a plausible preferred binding site in both fibril types. The ThT lifetime difference that we report here could therefore be a consequence of small geometric differences to this channel; these could be induced by for example variations in microstructure of the fibril core related to the two extra C-terminal residues in Aβ(1-42), or due to differences in the packing of protofilaments into the mature fibrils, as suggested by our AFM data. Small changes to the geometry of the ThT binding site (without disrupting its ThT-binding nature) will influence the rotational freedom of the bound ThT molecule, giving a photophysical explanation to the observed fluorescence lifetime difference.

In conclusion, this study reveals that differences in the architecture of Aβ fibrils can be detected and rationalised by the fluorescence properties of bound ThT, highlighting that this dye can be utilized, beyond its standard application in kinetic experiments, to obtain detailed information on the properties of amyloid fibrils related to disease.

Conflict of interest

None.

Acknowledgments

We thank Prof. Bo Albinsson for help with TCSPC data analysis. This study was supported by grants to E.K.E. from the Swedish Research Council (VR), the Wenner-Gren foundation, and Sweden's Innovation Agency (Vinnova). F.W. is funded by the Chalmers Area of Advance in Nanoscience and Nanotechnology and VR.

Appendix A. Supplementary data

Supplementary data related to this article can be found at http://dx.doi.org/10.1016/j.bbrc.2015.01.132.

Transparency document

Transparency document related to this article can be found online at http://dx.doi.org/10.1016/j.bbrc.2015.01.132.

References

[1] F. Chiti, C.M. Dobson, Protein misfolding, functional amyloid, and human disease, Annu Rev. Biochem. 75 (2006) 333–366.
[2] G.G. Glenner, C.W. Wong, Alzheimer's disease: initial report of the purification and characterization of a novel cerebrovascular amyloid protein, Biochem. Biophys. Res. Commun. 120 (1984) 885–890.
[3] H. Mori, K. Takio, M. Ogawara, et al., Mass spectrometry of purified amyloid beta protein in Alzheimer's disease, J. Biol. Chem. 267 (1992) 17082–17086.
[4] A.E. Roher, J.D. Lowenson, S. Clarke, et al., Structural alterations in the peptide backbone of beta-amyloid core protein may account for its deposition and stability in Alzheimer's disease, J. Biol. Chem. 268 (1993) 3072–3083.
[5] M. Sunde, L.C. Serpell, M. Bartlam, et al., Common core structure of amyloid fibrils by synchrotron X-ray diffraction, J. Mol. Biol. 273 (1997) 729–739.
[6] H. LeVine 3rd, Thioflavine T interaction with synthetic Alzheimer's disease beta-amyloid peptides: detection of amyloid aggregation in solution, Protein Sci. 2 (1993) 404–410.
[7] M. Groenning, Binding mode of Thioflavin T and other molecular probes in the context of amyloid fibrils-current status, J. Chem. Biol. 3 (2010) 1–18.
[8] M.R. Krebs, E.H. Bromley, A.M. Donald, The binding of thioflavin-T to amyloid fibrils: localisation and implications, J. Struct. Biol. 149 (2005) 30–37.
[9] M. Biancalana, K. Makabe, A. Koide, et al., Molecular Mechanism of Thioflavin-T binding to the surface of beta-rich peptide self-assemblies, J. Mol. Biol. 385 (2009) 1052–1063.
[10] L.S. Wolfe, M.F. Calabrese, A. Nath, et al., Protein-induced photophysical changes to the amyloid indicator dye thioflavin T, Proc. Natl. Acad. Sci. U S A 107 (2010) 16863–16868.
[11] M. Harel, L.K. Sonoda, I. Silman, et al., Crystal structure of thioflavin T bound to the peripheral site of Torpedo californica acetylcholinesterase reveals how thioflavin T acts as a sensitive fluorescent reporter of ligand binding to the acylation site, J. Am. Chem. Soc. 130 (2008) 7856–7861.
[12] M. Biancalana, S. Koide, Molecular mechanism of Thioflavin-T binding to amyloid fibrils, Biochim. Biophys. Acta 1804 (2010) 1405–1412.
[13] A.I. Sulatskaya, A.A. Maskevich, I.M. Kuznetsova, et al., Fluorescence quantum yield of thioflavin T in rigid isotropic solution and incorporated into the amyloid fibrils, PLoS One 5 (2010) e15385.
[14] E. Voropai, M. Samtsov, K. Kaplevskii, et al., Spectral properties of thioflavin T and its complexes with amyloid fibrils, J. Appl. Spectrosc. 70 (2003) 868–874.
[15] V.I. Stsiapura, A.A. Maskevich, V.A. Kuzmitsky, et al., Thioflavin T as a molecular rotor: fluorescent properties of thioflavin T in solvents with different viscosity, J. Phys. Chem. B 112 (2008) 15893–15902.
[16] J. Adler, H.A. Scheidt, M. Kruger, et al., Local interactions influence the fibrillation kinetics, structure and dynamics of Abeta(1-40) but leave the general fibril structure unchanged, Phys. Chem. Chem. Phys. 16 (2014) 7461–7471.
[17] D.M. Walsh, E. Thulin, A.M. Minogue, et al., A facile method for expression and purification of the Alzheimer's disease-associated amyloid beta-peptide, FEBS J. 276 (2009) 1266–1281.
[18] S.I. Cohen, S. Linse, L.M. Luheshi, et al., Proliferation of amyloid-beta42 aggregates occurs through a secondary nucleation mechanism, Proc. Natl. Acad. Sci. U S A 110 (2013) 9758–9763.
[19] B. Bolognesi, S.I. Cohen, P. Aran Terol, et al., Single point mutations induce a switch in the molecular mechanism of the aggregation of the Alzheimer's disease associated Abeta42 peptide, ACS Chem. Biol. 9 (2014) 378–382.
[20] A. Olofsson, A.E. Sauer-Eriksson, A. Ohman, The solvent protection of alzheimer amyloid-beta-(1-42) fibrils as determined by solution NMR spectroscopy, J. Biol. Chem. 281 (2006) 477–483.
[21] A. Olofsson, M. Lindhagen-Persson, A.E. Sauer-Eriksson, et al., Amide solvent protection analysis demonstrates that amyloid-beta(1-40) and amyloid-beta(1-42) form different fibrillar structures under identical conditions, Biochem. J. 404 (2007) 63–70.
[22] I. Kheterpal, M. Chen, K.D. Cook, et al., Structural differences in Abeta amyloid protofibrils and fibrils mapped by hydrogen exchange–mass spectrometry with on-line proteolytic fragmentation, J. Mol. Biol. 361 (2006) 785–795.
[23] A.T. Petkova, Y. Ishii, J.J. Balbach, et al., A structural model for Alzheimer's beta -amyloid fibrils based on experimental constraints from solid state NMR, Proc. Natl. Acad. Sci. U S A 99 (2002) 16742–16747.
[24] A.T. Petkova, W.M. Yau, R. Tycko, Experimental constraints on quaternary structure in Alzheimer's beta-amyloid fibrils, Biochemistry 45 (2006) 498–512.
[25] T. Luhrs, C. Ritter, M. Adrian, et al., 3D structure of Alzheimer's amyloid-beta(1-42) fibrils, Proc. Natl. Acad. Sci. U S A 102 (2005) 17342–17347.
[26] M. Torok, S. Milton, R. Kayed, et al., Structural and dynamic features of Alzheimer's Abeta peptide in amyloid fibrils studied by site-directed spin labeling, J. Biol. Chem. 277 (2002) 40810–40815.
[27] M. Fandrich, M. Schmidt, N. Grigorieff, Recent progress in understanding Alzheimer's beta-amyloid structures, Trends Biochem. Sci. 36 (2011) 338–345.
[28] T. Yamaguchi, H. Yagi, Y. Goto, et al., A disulfide-linked amyloid-beta peptide dimer forms a protofibril-like oligomer through a distinct pathway from amyloid fibril formation, Biochemistry 49 (2010) 7100–7107.
[29] W.F. Xue, A.L. Hellewell, W.S. Gosal, et al., Fibril fragmentation enhances amyloid cytotoxicity, J. Biol. Chem. 284 (2009) 34272–34282.
[30] G. Meisl, X. Yang, E. Hellstrand, et al., Differences in nucleation behavior underlie the contrasting aggregation kinetics of the Abeta40 and Abeta42 peptides, Proc. Natl. Acad. Sci. U S A 111 (2014) 9384–9389.
[31] C. Haupt, M. Bereza, S.T. Kumar, et al., Pattern recognition with a fibril-specific antibody fragment reveals the surface variability of natural amyloid fibrils, J. Mol. Biol. 408 (2011) 529–540.
[32] T. Klingstedt, K.P. Nilsson, Conjugated polymers for enhanced bioimaging, Biochim. Biophys. Acta 1810 (2011) 286–296.
[33] R. Sabate, I. Lascu, S.J. Saupe, On the binding of Thioflavin-T to HET-s amyloid fibrils assembled at pH 2, J. Struct. Biol. 162 (2008) 387–396.
[34] C. Wu, Z.X. Wang, H.X. Lei, et al., The binding of thioflavin t and its neutral analog BTA-1 to protofibrils of the Alzheimer's disease Abeta(16-22) peptide probed by molecular dynamics simulations, J. Mol. Biol. 384 (2008) 718–729.